# Journal Pre-proof

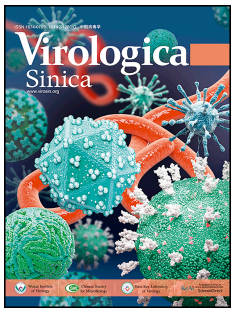


Mast cell degranulation-triggered by SARS-CoV-2 induces tracheal-bronchial epithelial inflammation and injury

Jian-Bo Cao, Shu-Tong Zhu, Xiao-Shan Huang, Xing-Yuan Wang, Meng-Li Wu, Xin-Li, Feng-Liang Liu, Ling Chen, Yong-Tang Zheng, Jian-Hua Wang

PII: S1995-820X(24)00027-0

DOI: https://doi.org/10.1016/j.virs.2024.03.001

Reference: VIRS 260

To appear in: *Virologica Sinica*

Received Date: 11 August 2023

Accepted Date: 27 February 2024

Please cite this article as: Cao, J.-B., Zhu, S.-T., Huang, X.-S., Wang, X.-Y., Wu, M.-L., Xin-Li, Liu, F.-L., Chen, L., Zheng, Y.-T., Wang, J.-H., Mast cell degranulation-triggered by SARS-CoV-2 induces tracheal-bronchial epithelial inflammation and injury, *Virologica Sinica*, https://doi.org/10.1016/j.virs.2024.03.001.

**VS-6474**

Received: 11 August 2023, Accepted: 27 February 2024

**RESEARCH ARTICLE**

# Mast cell degranulation-triggered by SARS-CoV-2 induces tracheal-bronchial epithelial inflammation and injury

Jian-Bo Cao [a, b, 1], Shu-Tong Zhu [a, 1], Xiao-Shan Huang [a, 1], Xing-Yuan Wang [a], Meng-Li Wu [a], Xin-Li [a], Feng-Liang Liu [c], Ling Chen [a], Yong-Tang Zheng [c,*], Jian-Hua Wang [a, d, *]

[a] Guangzhou Institutes of Biomedicine and Health, Chinese Academy of Sciences, Guangzhou 510530, China;
[b] School of Life Sciences and Medicine, University of Science and Technology of China, Hefei 230026, China.
[c] Key Laboratory of Bioactive Peptides of Yunnan Province, Key Laboratory of Animal Models and Human Disease Mechanisms of the Chinese Academy of Sciences, KIZ-CUHK Joint Laboratory of Bioresources and Molecular Research in Common Diseases, Center for Biosafety Mega-Science, Kunming Institute of Zoology, Chinese Academy of Sciences, Kunming 650223, China
[d] University of Chinese Academy of Sciences, Beijing 100039, China.

[1]Jian-Bo Cao, Shu-Tong Zhu, and Xiao-Shan Huang contribute equally.

***Correspondence authors**
Email: wang_jianhua@gibh.ac.cn (J.-H, Wang); zhengyt@mail.kiz.ac.cn (Y.-T Zheng)
ORCID: 0000-0002-6435-9907 (J.-H, Wang), 0000-0001-5469-0324 (Y.-T Zheng)

**Highlights**

1. SARS-CoV-2 infection induces mast cell accumulation and degranulation in the peri-trachea in mice.
2. Mast cell activation induces the production of inflammatory factors in bronchial epithelial cells.
3. Ebastine or loratadine reduces the induction of inflammatory factors and alleviate tracheal injury in mice.

**Abstract**

SARS-CoV-2 infection-induced hyper-inflammation is a key pathogenic factor of COVID-19. Our research, along with others', has demonstrated that mast cells (MCs) play a vital role in the initiation of hyper-inflammation caused by SARS-CoV-2. In previous study, we observed that SARS-CoV-2 infection the accumulation of MCs in the peri-bronchus and bronchioalveolar-duct junction in humanized mice. Additionally, we found that MC degranulation triggered by the spike protein- resulted in inflammation in alveolar epithelial cells and capillary endothelial cells, leading to subsequent lung injury. The trachea and bronchus are the route for SARS-CoV-2 transmission after virus inhalation, and inflammation in these regions could promote viral spread. MCs are widely distributed throughout the respiratory tract. Thus, in this study, we investigated the role of MCs and their degranulation in the development of inflammation in tracheal-bronchial epithelium. Histological analyses showed the accumulation and degranulation of MCs in the peri-trachea of humanized mice infected with SARS-CoV-2. MC degranulation caused lesions in trachea and the formation of papillary hyperplasia was observed. Through transcriptome analysis in bronchial epithelial cells, we found that MC degranulation significantly altered multiple cellular signaling, particularly, leading to upregulated immune responses and inflammation. The administration of ebastine or loratadine effectively suppressed the induction of inflammatory factors in bronchial epithelial cells and alleviated tracheal injury in mice. Taken together, our findings confirm the essential role of MC degranulation in SARS-CoV-2-induced hyper-inflammation and the subsequent tissue lesions. Furthermore, our results support the use of ebastine or loratadine to inhibit SARS-CoV-2-triggered degranulation, thereby preventing tissue damage caused by hyper-inflammation.

**Key words**: SARS-CoV-2, Mast cell (MC), Bronchial epithelial cell, Inflammation, Tracheal injury

## 1. Introduction

The coronavirus disease 2019 (COVID-19) caused by SARS-CoV-2 infection has led to a significant impact on global public health (Jiang and Shi, 2020; Wu et al., 2020; Zhou et al., 2020). A key pathologic feature of COVID-19 is the induction of hyper-inflammatory response, resulting in uncontrolled production of inflammatory cytokines and chemokines, leading to multi-organ failure, especially in the aged population and individuals with co-morbidities (Carsana et al., 2020; Guan et al., 2020; Mehta et al., 2020a; Mehta et al., 2020b; Dries, 2021; Song et al., 2021; Stein et al., 2022). Systemic inflammation is considered the primary pathophysiological factor for COVID-19 sequelae (Mehandru and Merad, 2022; Ryan et al., 2022; Altmann et al., 2023; Chaves et al., 2023; Marshall, Jr., 2023; Mohandas et al., 2023). However, the mechanisms underlying the induction of inflammation remain to be elucidated.

SARS-CoV-2 is predominantly transmitted via inhalation of respiratory droplets from infected individuals (Li et al., 2022). The epithelium of the nasal cavities, trachea, and large and small airways express high levels of viral receptor ACE2 (angiotensin converting-enzyme-2), and ACE2 expression increases in the elderly, smokers, and patients with chronic lung diseases (Leung et al., 2020; Baker et al., 2021; Bui et al., 2021). We and others have demonstrated the widespread distribution of SARS-CoV-2 virions in the peri-bronchus and bronchioalveolar-duct junction (Gu et al., 2020; Jiang et al., 2020; Wu et al., 2021). The tracheal-bronchial epithelium lining consists mainly of ciliated cells, secretory goblets, and basal cells. Among those, the ciliated cells express abundant ACE2 molecules and are most susceptible to SARS-CoV-2 infection (Hou et al., 2020b; Ahn et al., 2021; Khan et al., 2021). These infected ciliated cells can produce and shed multiple viral particles, which can move deeper into the lungs through inhalation (Robinot et al., 2021; Morrison et al., 2022). These tracheal-bronchial epithelial cells can be hyperactivated by SARS-CoV-2, leading to release of massive amounts of cytokines that triggered hyperactivation of leukocytes, hyper-inflammation, and tissue damage. Multiple desquamated bronchial epithelial cells were visible in the bronchial lumens in autopsies of COVID-19 patients. Ciliary impairment is accompanied by the axoneme loss and basal body misorientation (Potashnikova et al., 2023). SARS-CoV-2 replication leads to a rapid loss of the ciliary layer and impairs mucociliary clearance in a reconstructed human bronchial epithelium model (Robinot et al., 2021). Pathological phenomena, such as open intrapulmonary bronchopulmonary anastomoses, bronchial arteries enlargement, bronchopulmonary fistula and airway fibrin cast obstruction have been identified in COVID-19 patients (Barral et al., 2020; Galambos et al., 2021; Malkoc et al., 2022; Bodmer et al., 2023). Uncovering these virus-host interactions and induction of inflammation in the trachea-bronchia regions helps to understand viral spread and pathogenesis.

Mast cells (MCs) are tissue-resident cells strategically located throughout the host-environment interface, including the entire respiratory tract and the nasal cavity. In addition to being the main effector cells in type I allergic reactions, MCs are increasingly recognized for their regulatory roles in various pathophysiological processes (Elieh Ali Komi et al., 2020; Lam et al., 2021). In SARS-CoV-2 infection, MCs are massively recruited to the alveolar septa and pulmonary parenchyma in postmortem lung biopsies of COVID-19 patients or infected monkeys (Motta Junior et al., 2020; Ribeiro Dos Santos Miggiolaro et al., 2020; Malone et al., 2021; Budnevsky et al., 2022; Schaller et al., 2022). The severity of SARS-CoV-2 infection is associated with higher

numbers of alveolar MCs and greater degranulation (Krysko et al., 2022). Furthermore, the sera of post-acute sequelae of COVID-19 patients display a distinct profile of elevated inflammatory cytokines and MC-released proteases, suggesting an association between MC-induced systemic inflammation and long-COVID (Wechsler et al., 2022).

Recently, we discovered that SARS-CoV-2 infection led to the accumulation and degranulation of MCs in the peri-bronchus and bronchioalveolar-duct junction in humanized mice. The degranulation of MCs can induce the production of inflammatory factors in alveolar epithelial cells and capillary endothelial cells, resulting in lung injury (Wu et al., 2021; Wu et al., 2022). MC degranulation in the lungs of SARS-CoV-2-infected mice and nonhuman primates leads to lung inflammation and damages. Furthermore, the activation of lung MCs is significantly associated with disease severity in humans (Tan et al., 2023). The trachea and bronchus are the route for SARS-CoV-2 transmission through inhalation, and inflammation in these regions may facilitate viral invasion and spread. In our previous study, we have demonstrated that the interaction between the spike protein and the ACE2 receptor can induce MC degranulation (Wu et al., 2021). The spike proteins are highly expressed in the respiratory tract epithelia of COVID-19 patients and contribute to the inflammatory response (Dorward et al., 2021). Therefore, in this study, we aimed to investigate the role of MC degranulation in inducing inflammation in the tracheal-bronchial epithelium.

## 2. Materials and Methods

### *2.1. Cell lines and virus strains*

Human bronchial epithelial cells BEAS-2B were purchased from the Meisen CTCC, Zhejiang, China and cultured in DMEM/F12 medium (Gibco, USA). The culture medium contains 10% fatal bovine serum (Gibco), 100 U/mL penicillin and 100 μg/mL streptomycin. The culture of LAD2 human mast cells was prepared according to the reference (Wu et al., 2021). Pseudotyped virus was generated by EZ Trans cell transfection reagent (Life iLab, AC04L082)-mediated co-transfection of HEK293T cells with the spike-expressing plasmid pcDNA3.1-2019-nCoV-S-IRES (strain 2019-nCoV WIV04) and pNL4-3. Luc. ΔR ΔE (Liu et al., 2020). These two plasmids are provided by Dr. Lu Lu (Fudan University, Shanghai, China). Harvested supernatants of transfected cells that contained viral particles were aliquoted and stored at −80 °C.

### *2.2. Mouse strains and infection experiments*

C57BL/6N-ACE2$^{em2(hACE2\text{-}WPRE,\ pgk\text{-}puro)/CCLA}$ mice (3–4 months old) were purchased from Guangzhou Institutes of Biomedicine and Health, Chinese Academy of Science (Liu et al., 2021). The mice were randomly assigned to each group. The mice (five for each group) were infected by nasal inhalation with SARS-CoV-2 (strain 107) ($5 \times 10^6$ $TCID_{50}$) for indicated times. Mock infection was established with the same amount of PBS. The 107 strain of SARS-CoV-2 (NMDC000HUI) was provided by Guangdong Provincial Center for Disease Control and Prevention, Guangdong Province of China (Song et al., 2020). For some mice, ebastine (5 mg/kg) or loratadine (10 mg/kg) (both from Sigma-Aldrich) was administered one day before infection, and the treatments continued daily throughout the infection. Pathological, virological and tracheal samples were collected on the day of euthanization.

*2.3. Histological analysis*

To analyze the tracheas of mice, tissues were fixed in zinc formalin and routine histology was performed. Tissue sections of approximately 4 μm were stained with Hematoxylin and Eosin (H.E.) or Toluidine blue (T. Blue). The pathological section scanning and image analysis system (Tissue FAXS Plus ST) was utilized to examine the sections.

*2.4. Real-time (RT-)PCR*

The total RNA of BEAS-2B cells was extracted using the Trizol reagent (Invitrogen, USA). cDNA was synthesized from purified RNA (1 μg) using HiScript III RT SuperMix for qPCR kit. Real-time PCR was carried out by using the SYBR qPCR Mix (Genestar, A33-101) with the following thermal cycling conditions: 95 °C for 30 s followed by 40 cycles consisting of 95 °C for 10 s, 60 °C for 30 s. The expression level of target mRNA was normalized to *GAPDH*. The primers used for RT-PCR are listed in Supplementary Table S1.

*2.5. RNA Sequencing and data analysis*

Total RNAs from treated BEAS-2B cells were extracted using Trizol (Invitrogen) according to the manufacturer's protocol, and ribosomal RNA removed using QIAseq FastSelect-rRNA HMR Kits (QIAGEN, Germany). Fragmented RNAs (average length approximately 200 bp) were subjected to first strand and second strand cDNA synthesis, followed by adaptor ligation and enrichment with a low-cycle according to the instructions of NEBNext UltraTM RNA Library Prep Kit for Illumina (NEB, USA). The purified library products were evaluated using the Agilent 2200 TapeStation and Qubit2.0 (Life Technologies, USA). The libraries were paired-end sequenced (PE150, Sequencing reads were 150 bp) at Guangzhou RiboBio Co., Ltd. (Guangzhou, China) using Illumina HiSeq 3000 platform. The data analysis was according to the reference (Wu et al., 2021).

*2.6. Statistical Analysis*

Graphpad Prism 8.0 was used for statistical analysis. The statistical significance of difference between intra-groups was determined through Student's unpaired *t*-test.

## 3. Results

### *3.1. SARS-CoV-2 infection induces MC accumulation and degranulation in the peri- trachea and causes lesions in hACE2-humanized mice*

In humanized mice, we have observed that SARS-CoV-2 infection could induce MC accumulation and degranulation in the peri-bronchus and bronchioalveolar-duct junction (Wu et al., 2021). To investigate whether the same phenomenon occurs in the trachea, the ACE-2-humanized mice C57BL/6N-ACE2$^{em2(hACE2\text{-}WPRE,\ pgk\text{-}puro)/CCLA}$ were intratracheally infected with SARS-CoV-2 (strain 107, $5 \times 10^6$ $TCID_{50}$), then euthanized at 5 days post-infection (dpi) for histological analysis of the trachea. Mock infection was performed using the same amount of PBS. MCs and their degranulation were indicated by metachromatic labeling with Toluidine blue (T. blue). Compared to the mock-infection group (Fig. 1A), the accumulation of MCs and the release of granules were observed in the peri-trachea at the 5 dpi (Fig. 1C, 1E). Trachea lesions around the areas of MC accumulation and degranulation were examined using Hematoxylin and Eosin (H.E.) staining. Compared to the

mock-infection control (Fig. 1B), trachea lesions such as papillary hyperplasia, infiltration of inflammatory cells (lymphocytes and monocytes), and hyperplasia of epithelial cells, were observed around the areas of MC accumulation and degranulation (Fig. 1D, Supplementary Fig. S1B). Notably, there was obvious papillary hyperplasia in the airway trachea, which is often associated with inflammatory response (Dunbar et al., 2016). The papillary hyperplasia count and MC count was calculated in the peri-trachea (Fig. 1F–G). Taken together, these results demonstrate the accumulation and degranulation of MCs in the peri-trachea of SARS-CoV-2-infected mice, accompanied by obvious trachea lesions.

### *3.2. Transcriptome analysis reveals MC degranulation inducing remodeling of cellular signaling in human bronchial epithelial cell*

We previously demonstrated that the binding of spike/RBD protein with ACE2 receptor triggered MC degranulation in a LAD2 cell-based human MC model (Wu et al., 2021). We adopted this cell model to examine the effect of MC degranulation on the induction of inflammatory factors in human bronchial epithelial cell. SARS-CoV-2 spike/RBD protein was used to trigger degranulation in LAD2 cells, then the cell culture supernatants were harvested and used to treat the human bronchial epithelial cell BEAS-2B for 12 h. Then, BEAS-2B cells were collected and used for transcriptome analysis with standard protocols.

The volcano plot displayed a total of 519 up-regulated and 356 down-regulated genes in BEAS-2B cells upon treatment with spike/RBD-treated LAD2 cell culture supernatants (the sample "S"), compared to the group treated with normal cell culture supernatants (the sample "M") (Fig. 2A). To determine which genes were regulated by spike/RBD-induced MC degranulation, the GO analysis on up- and down-regulated genes was performed. The up-regulated genes were primarily associated with immune activity and inflammation reactions, such as inflammatory response regulation, immune effector processes, CXCR chemokine receptors binding, and granulocyte activation, etc. In contrast, the gene sets that regulate extracellular matrix organization, microtubule development, cell adhesion and cell migration were down-regulated (Fig. 2B). The gene set enrichment analysis (GAES) showed that the up-regulated genes were associated with regulating inflammatory responses and the SARS-CoV-2 life cycle, while the down-regulated genes were related to negative regulation of cell growth (Fig. 2C).

Transcription-factor enrichment showed that the differential expressed genes (DEGs) related to immune and inflammatory responses were up-regulated, e.g., *RELA*, *REL*, *NFKB1*, *STAT1*, *STAT3*, *SP1*, *PPARA*, *CEBP-β/δ*. The down-regulated transcription factors were mainly those governing cell growth and tumor formation, such as *ETS1*, *ARNTL*, *MYBL2*, *TP53* (Fig. 2D). The expression levels of inflammatory cytokines/chemokines increased substantially, among which the most increased were *IL-6*, *CSF1*, *CCL20*, *TNFSF14*, and *CXCL* chemokine family in cells (Fig. 2E). Genes governing the negative regulation of cell growth and the cell adhesion were significantly down-regulated including *NPPB*, *RGS4*, *SFRP2*, *NTM*, *BMP6* and *SEMA3E* (Fig. 2F and G). Genes involved in regulating the viral life cycle were also upregulated, and the most significantly up-regulated genes included *SLPI*, *CXCL8*, *PTX3*, *CCL2*, and *IL-32* (Fig. 2H). In addition, BEAS-2B cells express abundant ACE2 receptors and are susceptible to spike-pseudotyped viral infection (Supplementary Fig. S2).

Taken together, the transcriptome data reveals that spike/RBD-triggered MC degranulation has a significant impact on multiple cellular signaling in human bronchial epithelial cells. Specifically, MC degranulation upregulates immune responses and inflammation, while inhibits cellular signals involved in cell growth and adhesion.

### *3.3. Blocking MC activation hinders the induction of inflammatory factors*

Next, we went to confirm the induction of cytokine/chemokines in human bronchial epithelial cells following MC degranulation. The BEAS-2B cells were treated with LAD2/RBD co-culture supernatants (LAD2/RBD-supern.) or LAD2 cell normal culture supernatants (LAD2-supern.) for 12 h. Medium was used as mock control. The expressions of IL-6, IL-8, CCL20, CXCL10 and S100A9 were detected with real-time (RT-) PCR. The "LAD2/RBD-supern" induced a significantly high level expression of these cytokine/chemokines in BEAS-2B cells (Fig. 3A, 3B). The spontaneous or basal MC degranulation (the sample of "the LAD2-supern") resulted in minimal expressions of these cytokine/chemokines (Fig. 3A). In parallel, direct treatment of BEAS-2B cells with RBD proteins did not lead to any stimulation of these cytokine/chemokines (Fig. 3B).

We have previously reported that the compounds of ebastine (Eba.) or loratadine (Lor.) could reduce spike/RBD-induced MC degranulation (Wu et al., 2021; Wu et al., 2022). When treated with ebastine or loratadine, the capacity of cell culture supernatants from spike/RBD-treated MCs to induce IL-6, IL-8, CCL20, CXCL10 and S100A9 in BEAS-2B cells was significantly reduced (Fig. 3B). As a control, the direct treatment of BEAS-2B cells with Eba. or Lor., without additional degranulation stimulation did not affect cytokine expression (Supplementary Fig. S3).

Taken together, these data demonstrate that supernatants from spike/RBD treated MCs induce the expression of inflammatory factors in human bronchial epithelial cell. However, the treatment with ebastine or loratadine reduces the induction of inflammatory factors.

### *3.4. The induction of inflammatory factors by MC granules*

MC granules contain multiple biologic mediators, including histamine, serotonin, heparin, cytokine/chemokines, and enzymes such as chymase and tryptase, etc (Elieh Ali Komi et al., 2020). We have previously detected the rapid release of histamine, chymase and tryptase in SARS-CoV-2 (or spike/RBD)-treated LAD2 MC cells (Wu et al., 2021; Wu et al., 2022). The released histamine triggered by SARS-CoV-2 has been reported to induce high IL-1 levels, resulting in cytokine storm in COVID-19 patients (Conti et al., 2020). To profile the mediators-induced expression of inflammatory factors in human respiratory epithelial cells, the BEAS-2B cells were treated with histamine, chymase and tryptase for 12 h, respectively. The results showed that chymase and tryptase stimulated the expression of IL-6, IL-8, CCL20 and CXCL10, whereas, histamine induce preferentially S100A9 (Fig. 4).

### *3.5. The treatment with Lor. and Eba. reduces SARS-CoV-2-induced tracheal injury in mice*

We have previously demonstrated that the administration of ebastine or loratadine dampened SARS-CoV-2-induced production of inflammatory factors and thus prevented lung injury in mice (Wu et al., 2021; Wu et al., 2022). To determine whether the compounds play the same role in respiratory tract, we used the same SARS-

CoV-2 infection model based on hACE-2 humanized mice. The C57BL/6N-Ace2$^{em2(hACE2\text{-}WPRE,\ pgk\text{-}puro)/CCLA}$ were treated with Lor. (10 mg/kg) or Eba. (5 mg/kg) via intraperitoneal injection. one day prior to intranasal infection with SARS-CoV-2 (strain 107) at a dose of $5 \times 10^6$ $TCID_{50}$. Lor. or Eba. was administered daily until the mice were euthanized at 5 dpi. In SARS-CoV-2 infection group, MCs were accumulated in the peri-trachea. (Fig. 5A), and H.E. staining showed obvious papillary hyperplasia, epithelial cell hypertrophy and inflammatory cell infiltration in the trachea (Fig. 5B). The administration of Lor. and Eba. reduced MC accumulation and degranulation (Fig. 5C, 5E and 5G), and significantly reduced trachea lesions (Fig. 5D, 5F and 5H; Supplementary Fig. S1B–1D). Taken together, these results demonstrate that the treatment with Lor. and Eba. can reduce SARS-CoV-2-induced respiratory tract injury in mice.

## 4. Discussion

The mechanisms for SARS-CoV-2 induced hyper-inflammation remain to be elucidated, in which multiple cell types and cellular signaling pathways may be involved. The infected epithelial cells initiate a robust IFN response and release of inflammatory cytokines including IL-6 and IL-1β, which recruit and activate granulocytes, dendritic cells, and macrophages (Knoll et al., 2021; Luo et al., 2021; Ramasamy and Subbian, 2021; Zhang et al., 2021). SARS-CoV-2 stimulates monocytes from peripheral blood to elicit inflammatory responses through TNF-α, IL-1β and IL-6 (Codo et al., 2020; Boumaza et al., 2021). SARS-CoV-2 infection leads to cell death and systemic inflammation (Li et al., 2020; Zheng et al., 2021; Junqueira et al., 2022). Furthermore, the accumulation and excessive activation of macrophages in the lungs also contribute to local inflammation (Lee et al., 2021; Munnur et al., 2021).

By using the mouse and nonhuman primate infection models, we and others have demonstrated that rapid degranulation of lung mast cells induced by SARS-CoV-2 led to the production of inflammatory factors and subsequent lung injury (Wu et al., 2021; Wu et al., 2022; Tan et al., 2023). Activation of lung MCs is significantly associated with disease severity in humans (Tan et al., 2023). Considering the widespread presence of MCs throughout the host-environment interface, we speculate that SARS-CoV-2-induced MC degranulation represents a common mechanism for inducing hyper-inflammation. In this study, using cell and mouse models, we demonstrate that SARS-CoV-2-induced MC degranulation is a key intermediate step in the development of respiratory tract inflammation and subsequent lesions.

The large airways are preferred sites for viral transmission and replication (Hou et al., 2020a; Hou et al., 2020b). Infected ciliated cells in the trachea can be shed and serve as vehicles for viral spread (Zhu et al., 2020; Morrison et al., 2022). We observed that SARS-CoV-2 infection induced papillary hyperplasia in the tracheal mucosa of mice. The protruding papillary hyperplasia is likely to be a cell mass carrying multiple virus particles and easy to fall off. MC degranulation disrupts cell adhesion in respiratory tract epithelial cells, which may drive cell shedding and viral spread. Conversely, the administration of ebastine or loratadine can significantly reduce the production of inflammatory factors, prevent the disruption of cell adhesion (Wu et al., 2021; Wu et al., 2022), and minimize the formation of papillary hyperplasia in the trachea. Therefore, ebastine or loratadine may provide a clue for interference.

Upon activation by allergens or pathogens, MCs can rapidly release multiple mediators, such as histamine, tryptase, chymase, leukotrienes, cytokines, and chemokines, to regulate immune responses (Abraham and St John, 2010; Carroll-Portillo et al., 2012; Marshall et al., 2019). We have detected an abundant release of histamine, chymase and tryptase in SARS-CoV-2 (or spike/RBD)-treated LAD2 MC cells (Wu et al., 2021; Wu et al., 2022). In this study, we profiled the induction of inflammatory factors by MC released components. Meantime, compared to the stimulation with LAD2-degranulated supernatants, the stimulation with any component alone did not reach the same level, suggesting a potential synergy among various components during the induction of inflammatory factors. Additionally, these mediators may have multiple effects. For example, under inflammatory or pathological conditions, chymase can amplify local angiotensin-2 concentrations to cause leukocyte aggregation (Imai et al., 2005; Company et al., 2011).

## 5. Conclusion

In this study, we demonstrate that SARS-CoV-2 triggers MC activation and induces respiratory tract epithelial inflammation. The ebastine and loratadine should be evaluated for its potential clinical use for protecting tissue damage caused by hyper-inflammation.

## Data availability

The raw sequence data reported in this paper have been deposited in the Genome Sequence Archive (Genomics, Proteomics & Bioinformatics 2021) in National Genomics Data Center (Nucleic Acids Res 2022), China National Center for Bioinformation / Beijing Institute of Genomics, Chinese Academy of Sciences (GSA-Human: HRA005189) that are publicly accessible at https://ngdc.cncb.ac.cn/gsa-human.

## Ethics statement

All animal experiments were approved by the Institutional Animal Care and Use Committee of Guangzhou Institutes of Biomedicine and Health, Chinese Academy of Sciences (approval No. N2021016). The SARS-CoV-2 animal model experiments and protocols were discussed explicitly and extensively with biosafety officers and facility managers. All animal experiments and wild type virus were conducted within the animal biosafety level 3 (ABSL-3) facility in the National Kunming High-Level Biosafety Primate Laboratory Center. All experiments were performed in accordance with relevant guidelines and regulations.

## Author Contributions

Jian-Bo Cao, Xiao-Shan Huang, Shu-Tong Zhu: Data curation, Formal analysis, Methodology, Investigation, Software, Visualization, original draft; Meng-Li Wu, Xing-Yuan Wang, Xin-Li, Feng-Liang Liu: Investigation, Visualization; Ling Chen: Resources, Validation; Yong-Tang Zheng: Project administration, Resources, Validation, Funding acquisition; Jian-Hua Wang: Project administration, Supervision, original draft, review & editing, Funding acquisition;

## Conflict of interest

The authors declare no conflict of interest. Prof. Ling Chen and Prof. Jian-Hua Wang are editorial board members for *Virologica Sinica* and were not involved in the editorial review or the decision to publish this article.

## Acknowledgements

We thank ABSL-3 staffs and Dr. Lu Lu for kind gift of reagents, and thank Dr. Xia Jin for language editing. This work was supported by the National Natural Science Foundation of China (82172242), the Natural Science Foundation of Guangdong (2022A1515012053), National Key Research and Development Program of China (2022YFC2303700, 2021YFE0113000), Yunnan Key Research and Development Program (202103AC100005), the State key Laboratory of Respiratory Disease, Guangzhou, China (SKLRD-OP202207). The funders had no role in study design, data collection and analysis, decision to publish, or preparation of the manuscript.

## Appendix A. Supplementary data

Supplementary data to this article can be found online at https://doi.org/10.1016/j.virs.####

## References

Abraham, S.N., St John, A.L., 2010. Mast cell-orchestrated immunity to pathogens. Nat Rev Immunol, 10, 440-452.

Ahn, J.H., Kim, J., Hong, S.P., Choi, S.Y., Yang, M.J., Ju, Y.S., Kim, Y.T., Kim, H.M., Rahman, M.D.T., Chung, M.K., Hong, S.D., Bae, H., Lee, C.S., Koh, G.Y., 2021. Nasal ciliated cells are primary targets for SARS-CoV-2 replication in the early stage of COVID-19. J Clin Invest, 131, e148517.

Altmann, D.M., Whettlock, E.M., Liu, S., Arachchillage, D.J., Boyton, R.J., 2023. The immunology of long COVID. Nat Rev Immunol 23,618-634.

Baker, S.A., Kwok, S., Berry, G.J., Montine, T.J., 2021. Angiotensin-converting enzyme 2 (ACE2) expression increases with age in patients requiring mechanical ventilation. PLoS One, 16, e0247060.

Barral, M., Sirol, M., El Hajjam, M., Zhang, N., Petit, A., Cornelis, F.H., 2020. Bronchial Artery Embolization Performed in COVID-19 Patients: Tolerance and Outcomes. Cardiovasc Intervent Radiol, 43, 1949-1951.

Bodmer, J.L., Weinman, J., Veress, L.A., Galambos, C., 2023. Obstructive Bronchial Fibrin Cast Formation in COVID-19 Severe Respiratory Failure. Am J Respir Crit Care Med, 207, 349-350.

Boumaza, A., Gay, L., Mezouar, S., Bestion, E., Diallo, A.B., Michel, M., Desnues, B., Raoult, D., La Scola, B., Halfon, P., Vitte, J., Olive, D., Mege, J.L., 2021. Monocytes and Macrophages, Targets of Severe Acute Respiratory Syndrome Coronavirus 2: The Clue for Coronavirus Disease 2019 Immunoparalysis. J Infect Dis, 224, 395-406.

Budnevsky, A.V., Avdeev, S.N., Kosanovic, D., Shishkina, V.V., Filin, A.A., Esaulenko, D.I., Ovsyannikov, E.S., Samoylenko, T.V., Redkin, A.N., Suvorova, O.A., Perveeva, I.M., 2022. Role of mast cells in the pathogenesis of severe lung damage in COVID-19 patients. Respir Res, 23, 371.

Bui, L.T., Winters, N.I., Chung, M.I., Joseph, C., Gutierrez, A.J., Habermann, A.C., Adams, T.S., Schupp, J.C., Poli, S., Peter, L.M., Taylor, C.J., Blackburn, J.B., Richmond, B.W., Nicholson, A.G., Rassl, D., Wallace, W.A., Rosas, I.O., Jenkins, R.G., Kaminski, N., Kropski, J.A., Banovich, N.E., Human Cell Atlas Lung Biological, N., 2021. Chronic lung diseases are associated with gene expression programs favoring SARS-CoV-2 entry and severity. Nat Commun, 12, 4314.

Carroll-Portillo, A., Surviladze, Z., Cambi, A., Lidke, D.S., Wilson, B.S., 2012. Mast cell synapses and exosomes: membrane contacts for information exchange. Front Immunol, 3, 46.

Carsana, L., Sonzogni, A., Nasr, A., Rossi, R.S., Pellegrinelli, A., Zerbi, P., Rech, R., Colombo, R., Antinori, S., Corbellino, M., Galli, M., Catena, E., Tosoni, A., Gianatti, A., Nebuloni, M., 2020. Pulmonary post-mortem findings in a series of COVID-19 cases from northern Italy: a two-centre descriptive study. Lancet Infect Dis, 20, 1135-1140.

Chaves, A.M., Braniff, O., Angelova, A., Deng, Y., Tremblay, M.E., 2023. Chronic inflammation, neuroglia dysfunction, and plasmalogen deficiency as a new pathobiological hypothesis addressing the overlap between post-COVID-19 symptoms and myalgic encephalomyelitis/chronic fatigue syndrome. Brain Res Bull, 201, 110702.

Codo, A.C., Davanzo, G.G., Monteiro, L.B., De Souza, G.F., Muraro, S.P., Virgilio-Da-Silva, J.V., Prodonoff, J.S., Carregari, V.C., De Biagi Junior, C.a.O., Crunfli, F., Jimenez Restrepo, J.L., Vendramini, P.H., Reis-De-Oliveira, G., Bispo Dos Santos, K., Toledo-Teixeira, D.A., Parise, P.L., Martini, M.C., Marques, R.E., Carmo, H.R., Borin, A., Coimbra, L.D., Boldrini, V.O., Brunetti, N.S., Vieira, A.S., Mansour, E., Ulaf, R.G., Bernardes, A.F., Nunes, T.A., Ribeiro, L.C., Palma, A.C., Agrela, M.V., Moretti, M.L., Sposito, A.C., Pereira, F.B., Velloso, L.A., Vinolo, M.a.R., Damasio, A., Proença-Módena, J.L., Carvalho, R.F., Mori, M.A., Martins-De-Souza, D., Nakaya, H.I., Farias, A.S., Moraes-Vieira, P.M., 2020. Elevated Glucose Levels Favor SARS-CoV-2 Infection and Monocyte Response through a HIF-1α/Glycolysis-Dependent Axis. Cell Metab, 32, 437-446.e435.

Company, C., Piqueras, L., Naim Abu Nabah, Y., Escudero, P., Blanes, J.I., Jose, P.J., Morcillo, E.J., Sanz, M.J., 2011. Contributions of ACE and mast cell chymase to endogenous angiotensin II generation and leucocyte recruitment in vivo. Cardiovasc Res, 92, 48-56.

Conti, P., Caraffa, A., Tete, G., Gallenga, C.E., Ross, R., Kritas, S.K., Frydas, I., Younes, A., Di Emidio, P., Ronconi, G., 2020. Mast cells activated by SARS-CoV-2 release histamine which increases IL-1 levels causing cytokine storm and inflammatory reaction in COVID-19. J Biol Regul Homeost Agents, 34, 1629-1632.

Dorward, D.A., Russell, C.D., Um, I.H., Elshani, M., Armstrong, S.D., Penrice-Randal, R., Millar, T., Lerpiniere, C.E.B., Tagliavini, G., Hartley, C.S., Randle, N.P., Gachanja, N.N., Potey, P.M.D., Dong, X., Anderson, A.M., Campbell, V.L., Duguid, A.J., Al Qsous, W., Bouhaidar, R., Baillie, J.K., Dhaliwal, K., Wallace, W.A., Bellamy, C.O.C., Prost, S., Smith, C., Hiscox, J.A., Harrison, D.J., Lucas, C.D., 2021. Tissue-Specific Immunopathology in Fatal COVID-19. Am J Respir Crit Care Med, 203, 192-201.

Dries, D.J., 2021. Coronavirus Disease 2019: From Intensive Care Unit to the Long Haul-Part 2. Air Med J, 40, 298-302.

Dunbar, K.B., Agoston, A.T., Odze, R.D., Huo, X., Pham, T.H., Cipher, D.J., Castell, D.O., Genta, R.M., Souza, R.F., Spechler, S.J., 2016. Association of Acute Gastroesophageal Reflux Disease With Esophageal Histologic Changes. Jama, 315, 2104-2112.

Elieh Ali Komi, D., Wohrl, S., Bielory, L., 2020. Mast Cell Biology at Molecular Level: a Comprehensive Review. Clin Rev Allergy Immunol, 58, 342-365.

Galambos, C., Bush, D., Abman, S.H., 2021. Intrapulmonary bronchopulmonary anastomoses in COVID-19 respiratory failure. Eur Respir J, 58, 2004397.

Gu, H., Chen, Q., Yang, G., He, L., Fan, H., Deng, Y.Q., Wang, Y., Teng, Y., Zhao, Z., Cui, Y., Li, Y., Li, X.F., Li, J., Zhang, N.N., Yang, X., Chen, S., Guo, Y., Zhao, G., Wang, X., Luo, D.Y., Wang, H., Yang, X., Li, Y., Han, G., He, Y., Zhou, X., Geng, S., Sheng, X., Jiang, S., Sun, S., Qin, C.F., Zhou, Y., 2020. Adaptation of SARS-CoV-2 in BALB/c mice for testing vaccine efficacy. Science, 369, 1603-1607.

Guan, W.J., Liang, W.H., Zhao, Y., Liang, H.R., Chen, Z.S., Li, Y.M., Liu, X.Q., Chen, R.C., Tang, C.L., Wang, T., Ou, C.Q., Li, L., Chen, P.Y., Sang, L., Wang, W., Li, J.F., Li, C.C., Ou, L.M., Cheng, B., Xiong, S., Ni, Z.Y., Xiang, J., Hu, Y., Liu, L., Shan, H., Lei, C.L., Peng, Y.X., Wei, L., Liu, Y., Hu, Y.H., Peng, P., Wang, J.M., Liu, J.Y., Chen, Z., Li, G., Zheng, Z.J., Qiu, S.Q., Luo, J., Ye, C.J., Zhu, S.Y., Cheng, L.L., Ye, F., Li, S.Y., Zheng, J.P., Zhang, N.F., Zhong, N.S., He, J.X., 2020. Comorbidity and its impact on 1590 patients with COVID-19 in China: a

397 nationwide analysis. Eur Respir J, 55, 2000547.
398 Hou, Y.J., Chiba, S., Halfmann, P., Ehre, C., Kuroda, M., Dinnon, K.H., 3rd, Leist, S.R., Schäfer, A., Nakajima, N.,
399 Takahashi, K., Lee, R.E., Mascenik, T.M., Graham, R., Edwards, C.E., Tse, L.V., Okuda, K., Markmann, A.J.,
400 Bartelt, L., De Silva, A., Margolis, D.M., Boucher, R.C., Randell, S.H., Suzuki, T., Gralinski, L.E., Kawaoka, Y.,
401 Baric, R.S., 2020a. SARS-CoV-2 D614G variant exhibits efficient replication ex vivo and transmission in vivo.
402 Science, 370, 1464-1468.
403 Hou, Y.J., Okuda, K., Edwards, C.E., Martinez, D.R., Asakura, T., Dinnon, K.H., 3rd, Kato, T., Lee, R.E., Yount, B.L.,
404 Mascenik, T.M., Chen, G., Olivier, K.N., Ghio, A., Tse, L.V., Leist, S.R., Gralinski, L.E., Schäfer, A., Dang, H.,
405 Gilmore, R., Nakano, S., Sun, L., Fulcher, M.L., Livraghi-Butrico, A., Nicely, N.I., Cameron, M., Cameron, C.,
406 Kelvin, D.J., De Silva, A., Margolis, D.M., Markmann, A., Bartelt, L., Zumwalt, R., Martinez, F.J., Salvatore, S.P.,
407 Borczuk, A., Tata, P.R., Sontake, V., Kimple, A., Jaspers, I., O'neal, W.K., Randell, S.H., Boucher, R.C., Baric,
408 R.S., 2020b. SARS-CoV-2 Reverse Genetics Reveals a Variable Infection Gradient in the Respiratory Tract. Cell,
409 182, 429-446.e414.
410 Imai, Y., Kuba, K., Rao, S., Huan, Y., Guo, F., Guan, B., Yang, P., Sarao, R., Wada, T., Leong-Poi, H., Crackower, M.A.,
411 Fukamizu, A., Hui, C.C., Hein, L., Uhlig, S., Slutsky, A.S., Jiang, C., Penninger, J.M., 2005. Angiotensin-
412 converting enzyme 2 protects from severe acute lung failure. Nature, 436, 112-116.
413 Jiang, R.D., Liu, M.Q., Chen, Y., Shan, C., Zhou, Y.W., Shen, X.R., Li, Q., Zhang, L., Zhu, Y., Si, H.R., Wang, Q., Min, J.,
414 Wang, X., Zhang, W., Li, B., Zhang, H.J., Baric, R.S., Zhou, P., Yang, X.L., Shi, Z.L., 2020. Pathogenesis of
415 SARS-CoV-2 in Transgenic Mice Expressing Human Angiotensin-Converting Enzyme 2. Cell, 182, 50-58 e58.
416 Jiang, S., Shi, Z.L., 2020. The First Disease X is Caused by a Highly Transmissible Acute Respiratory Syndrome
417 Coronavirus. Virol Sin, 35, 263-265.
418 Junqueira, C., Crespo, Â., Ranjbar, S., De Lacerda, L.B., Lewandrowski, M., Ingber, J., Parry, B., Ravid, S., Clark, S.,
419 Schrimpf, M.R., Ho, F., Beakes, C., Margolin, J., Russell, N., Kays, K., Boucau, J., Das Adhikari, U., Vora, S.M.,
420 Leger, V., Gehrke, L., Henderson, L.A., Janssen, E., Kwon, D., Sander, C., Abraham, J., Goldberg, M.B., Wu, H.,
421 Mehta, G., Bell, S., Goldfeld, A.E., Filbin, M.R., Lieberman, J., 2022. FcγR-mediated SARS-CoV-2 infection of
422 monocytes activates inflammation. Nature, 606, 576-584.
423 Khan, M., Yoo, S.J., Clijsters, M., Backaert, W., Vanstapel, A., Speleman, K., Lietaer, C., Choi, S., Hether, T.D., Marcelis,
424 L., Nam, A., Pan, L., Reeves, J.W., Van Bulck, P., Zhou, H., Bourgeois, M., Debaveye, Y., De Munter, P., Gunst,
425 J., Jorissen, M., Lagrou, K., Lorent, N., Neyrinck, A., Peetermans, M., Thal, D.R., Vandenbriele, C., Wauters, J.,
426 Mombaerts, P., Van Gerven, L., 2021. Visualizing in deceased COVID-19 patients how SARS-CoV-2 attacks the
427 respiratory and olfactory mucosae but spares the olfactory bulb. Cell, 184, 5932-5949.e5915.
428 Knoll, R., Schultze, J.L., Schulte-Schrepping, J., 2021. Monocytes and Macrophages in COVID-19. Front Immunol, 12,
429 720109.
430 Krysko, O., Bourne, J.H., Kondakova, E., Galova, E.A., Whitworth, K., Newby, M.L., Bachert, C., Hill, H., Crispin, M.,
431 Stamataki, Z., Cunningham, A.F., Pugh, M., Khan, A.O., Rayes, J., Vedunova, M., Krysko, D.V., Brill, A., 2022.
432 Severity of SARS-CoV-2 infection is associated with high numbers of alveolar mast cells and their degranulation.
433 Front Immunol, 13, 968981.
434 Lam, H.Y., Tergaonkar, V., Kumar, A.P., Ahn, K.S., 2021. Mast cells: Therapeutic targets for COVID-19 and beyond.
435 IUBMB Life, 73, 1278-1292.
436 Lee, J.S., Koh, J.Y., Yi, K., Kim, Y.I., Park, S.J., Kim, E.H., Kim, S.M., Park, S.H., Ju, Y.S., Choi, Y.K., Park, S.H., 2021.
437 Single-cell transcriptome of bronchoalveolar lavage fluid reveals sequential change of macrophages during
438 SARS-CoV-2 infection in ferrets. Nat Commun, 12, 4567.
439 Leung, J.M., Yang, C.X., Tam, A., Shaipanich, T., Hackett, T.L., Singhera, G.K., Dorscheid, D.R., Sin, D.D., 2020. ACE-
440 2 expression in the small airway epithelia of smokers and COPD patients: implications for COVID-19. Eur Respir

J, 55, 2000688.

Li, J., Zhang, Y., Jiang, L., Cheng, H., Li, J., Li, L., Chen, Z., Tang, F., Fu, Y., Jin, Y., Lu, B., Zheng, J., Wang, Z., 2022. Similar aerosol emission rates and viral loads in upper respiratory tracts for COVID-19 patients with Delta and Omicron variant infection. Virol Sin, 37, 762-764.

Li, S., Zhang, Y., Guan, Z., Li, H., Ye, M., Chen, X., Shen, J., Zhou, Y., Shi, Z.L., Zhou, P.,Peng, K., 2020. SARS-CoV-2 triggers inflammatory responses and cell death through caspase-8 activation. Signal Transduct Target Ther, 5, 235.

Liu, F.L., Wu, K., Sun, J., Duan, Z., Quan, X., Kuang, J., Chu, S., Pang, W., Gao, H., Xu, L., Li, Y.C., Zhang, H.L., Wang, X.H., Luo, R.H., Feng, X.L., Schöler, H.R., Chen, X., Pei, D., Wu, G., Zheng, Y.T.,Chen, J., 2021. Rapid generation of ACE2 humanized inbred mouse model for COVID-19 with tetraploid complementation. Natl Sci Rev, 8, nwaa285.

Liu, Z., Xu, W., Xia, S., Gu, C., Wang, X., Wang, Q., Zhou, J., Wu, Y., Cai, X., Qu, D., Ying, T., Xie, Y., Lu, L., Yuan, Z., Jiang, S., 2020. RBD-Fc-based COVID-19 vaccine candidate induces highly potent SARS-CoV-2 neutralizing antibody response. Signal Transduct Target Ther, 5, 282.

Luo, W., Zhang, J.W., Zhang, W., Lin, Y.L., Wang, Q., 2021. Circulating levels of IL-2, IL-4, TNF-α, IFN-γ, and C-reactive protein are not associated with severity of COVID-19 symptoms. J Med Virol, 93, 89-91.

Malkoc, A., Gill, H., Liu, N., Nguyen, D.T., Phan, A.T., Nguyen, A., Toporoff, B., 2022. Bronchopulmonary Fistula Development in an Elderly Male With COVID-19 Infection. Cureus, 14, e31686.

Malone, R.W., Tisdall, P., Fremont-Smith, P., Liu, Y., Huang, X.P., White, K.M., Miorin, L., Moreno, E., Alon, A., Delaforge, E., Hennecker, C.D., Wang, G., Pottel, J., Blair, R.V., Roy, C.J., Smith, N., Hall, J.M., Tomera, K.M., Shapiro, G., Mittermaier, A., Kruse, A.C., Garcia-Sastre, A., Roth, B.L., Glasspool-Malone, J., Ricke, D.O., 2021. COVID-19: Famotidine, Histamine, Mast Cells, and Mechanisms. Front Pharmacol, 12, 633680.

Marshall, G.D., Jr., 2023. The pathophysiology of postacute sequelae of COVID-19 (PASC): Possible role for persistent inflammation. Asia Pac Allergy, 13, 77-84.

Marshall, J.S., Portales-Cervantes, L.,Leong, E., 2019. Mast Cell Responses to Viruses and Pathogen Products. Int J Mol Sci, 20, 4241.

Mehandru, S., Merad, M., 2022. Pathological sequelae of long-haul COVID. Nat Immunol, 23, 194-202.

Mehta, P., Mcauley, D.F., Brown, M., Sanchez, E., Tattersall, R.S., Manson, J.J., 2020a. COVID-19: consider cytokine storm syndromes and immunosuppression. Lancet, 395, 1033-1034.

Mehta, P., Porter, J.C., Manson, J.J., Isaacs, J.D., Openshaw, P.J.M., Mcinnes, I.B., Summers, C., Chambers, R.C., 2020b. Therapeutic blockade of granulocyte macrophage colony-stimulating factor in COVID-19-associated hyperinflammation: challenges and opportunities. Lancet Respir Med, 8, 822-830.

Mohandas, S., Jagannathan, P., Henrich, T.J., Sherif, Z.A., Bime, C., Quinlan, E., Portman, M.A., Gennaro, M., Rehman, J., Force, R.M.P.T., 2023. Immune mechanisms underlying COVID-19 pathology and post-acute sequelae of SARS-CoV-2 infection (PASC). Elife, 12, e86014.

Morrison, C.B., Edwards, C.E., Shaffer, K.M., Araba, K.C., Wykoff, J.A., Williams, D.R., Asakura, T., Dang, H., Morton, L.C., Gilmore, R.C., O'neal, W.K., Boucher, R.C., Baric, R.S., Ehre, C., 2022. SARS-CoV-2 infection of airway cells causes intense viral and cell shedding, two spreading mechanisms affected by IL-13. Proc Natl Acad Sci U S A, 119, e2119680119.

Motta Junior, J.D.S., Miggiolaro, A., Nagashima, S., De Paula, C.B.V., Baena, C.P., Scharfstein, J., De Noronha, L., 2020. Mast Cells in Alveolar Septa of COVID-19 Patients: A Pathogenic Pathway That May Link Interstitial Edema to Immunothrombosis. Front Immunol, 11, 574862.

Munnur, D., Teo, Q., Eggermont, D., Lee, H.H.Y., Thery, F., Ho, J., Van Leur, S.W., Ng, W.W.S., Siu, L.Y.L., Beling, A., Ploegh, H., Pinto-Fernandez, A., Damianou, A., Kessler, B., Impens, F., Mok, C.K.P., Sanyal, S., 2021. Altered ISGylation drives aberrant macrophage-dependent immune responses during SARS-CoV-2 infection. Nat

Immunol, 22, 1416-1427.

Potashnikova, D.M., Sotnikova, T.N., Shirokova, O.M., Zayratyants, O.V., Vasilieva, E.Y., Sheval, E.V., 2023. Cilia impairment in bronchial epithelial cells detected in autopsy material of SARS-CoV-2-infected patient. Ultrastruct Pathol, 47, 382-387.

Ramasamy, S., Subbian, S., 2021. Critical Determinants of Cytokine Storm and Type I Interferon Response in COVID-19 Pathogenesis. Clin Microbiol Rev, 34, e00299-20.

Ribeiro Dos Santos Miggiolaro, A.F., Da Silva Motta Junior, J., Busatta Vaz De Paula, C., Nagashima, S., Alessandra Scaranello Malaquias, M., Baena Carstens, L., A, N.M.-A., Pellegrino Baena, C., De Noronha, L., 2020. Covid-19 cytokine storm in pulmonary tissue: Anatomopathological and immunohistochemical findings. Respir Med Case Rep, 31, 101292.

Robinot, R., Hubert, M., De Melo, G.D., Lazarini, F., Bruel, T., Smith, N., Levallois, S., Larrous, F., Fernandes, J., Gellenoncourt, S., Rigaud, S., Gorgette, O., Thouvenot, C., Trebeau, C., Mallet, A., Dumenil, G., Gobaa, S., Etournay, R., Lledo, P.M., Lecuit, M., Bourhy, H., Duffy, D., Michel, V., Schwartz, O., Chakrabarti, L.A., 2021. SARS-CoV-2 infection induces the dedifferentiation of multiciliated cells and impairs mucociliary clearance. Nat Commun, 12, 4354.

Ryan, F.J., Hope, C.M., Masavuli, M.G., Lynn, M.A., Mekonnen, Z.A., Yeow, A.E.L., Garcia-Valtanen, P., Al-Delfi, Z., Gummow, J., Ferguson, C., O'connor, S., Reddi, B.a.J., Hissaria, P., Shaw, D., Kok-Lim, C., Gleadle, J.M., Beard, M.R., Barry, S.C., Grubor-Bauk, B., Lynn, D.J., 2022. Long-term perturbation of the peripheral immune system months after SARS-CoV-2 infection. BMC Med, 20, 26.

Schaller, T., Markl, B., Claus, R., Sholl, L., Hornick, J.L., Giannetti, M.P., Schweizer, L., Mann, M., Castells, M., 2022. Mast cells in lung damage of COVID-19 autopsies: A descriptive study. Allergy, 77, 2237-2239.

Song, T.Z., Zheng, H.Y., Han, J.B., Jin, L., Yang, X., Liu, F.L., Luo, R.H., Tian, R.R., Cai, H.R., Feng, X.L., Liu, C., Li, M.H., Zheng, Y.T., 2020. Delayed severe cytokine storm and immune cell infiltration in SARS-CoV-2-infected aged Chinese rhesus macaques. Zool Res, 41, 503-516.

Song, W.J., Hui, C.K.M., Hull, J.H., Birring, S.S., Mcgarvey, L., Mazzone, S.B., Chung, K.F., 2021. Confronting COVID-19-associated cough and the post-COVID syndrome: role of viral neurotropism, neuroinflammation, and neuroimmune responses. Lancet Respir Med, 9, 533-544.

Stein, S.R., Ramelli, S.C., Grazioli, A., Chung, J.Y., Singh, M., Yinda, C.K., Winkler, C.W., Sun, J., Dickey, J.M., Ylaya, K., Ko, S.H., Platt, A.P., Burbelo, P.D., Quezado, M., Pittaluga, S., Purcell, M., Munster, V.J., Belinky, F., Ramos-Benitez, M.J., Boritz, E.A., Lach, I.A., Herr, D.L., Rabin, J., Saharia, K.K., Madathil, R.J., Tabatabai, A., Soherwardi, S., Mccurdy, M.T., Peterson, K.E., Cohen, J.I., De Wit, E., Vannella, K.M., Hewitt, S.M., Kleiner, D.E., Chertow, D.S., 2022. SARS-CoV-2 infection and persistence in the human body and brain at autopsy. Nature, 612, 758-763.

Tan, J.Y., Anderson, D.E., Rathore, A.P., O'neill, A., Mantri, C.K., Saron, W.A., Lee, C.Q., Cui, C.W., Kang, A.E., Foo, R., Kalimuddin, S., Low, J.G., Ho, L., Tambyah, P., Burke, T.W., Woods, C.W., Chan, K.R., Karhausen, J., St John, A.L., 2023. Mast cell activation in lungs during SARS-CoV-2 infection associated with lung pathology and severe COVID-19. J Clin Invest, 133, e149834.

Wechsler, J.B., Butuci, M., Wong, A., Kamboj, A.P., Youngblood, B.A., 2022. Mast cell activation is associated with post-acute COVID-19 syndrome. Allergy, 77, 1288-1291.

Wu, F., Zhao, S., Yu, B., Chen, Y.M., Wang, W., Song, Z.G., Hu, Y., Tao, Z.W., Tian, J.H., Pei, Y.Y., Yuan, M.L., Zhang, Y.L., Dai, F.H., Liu, Y., Wang, Q.M., Zheng, J.J., Xu, L., Holmes, E.C., Zhang, Y.Z., 2020. A new coronavirus associated with human respiratory disease in China. Nature, 579, 265-269.

Wu, M.L., Liu, F.L., Sun, J., Li, X., He, X.Y., Zheng, H.Y., Zhou, Y.H., Yan, Q., Chen, L., Yu, G.Y., Chang, J., Jin, X., Zhao, J., Chen, X.W., Zheng, Y.T., Wang, J.H., 2021. SARS-CoV-2-triggered mast cell rapid degranulation

induces alveolar epithelial inflammation and lung injury. Signal Transduct Target Ther, 6, 428.

Wu, M.L., Liu, F.L., Sun, J., Li, X., Qin, J.R., Yan, Q.H., Jin, X., Chen, X.W., Zheng, Y.T., Zhao, J.C., Wang, J.H., 2022. Combinational benefit of antihistamines and remdesivir for reducing SARS-CoV-2 replication and alleviating inflammation-induced lung injury in mice. Zool Res, 43, 457-468.

Zhang, F., Mears, J.R., Shakib, L., Beynor, J.I., Shanaj, S., Korsunsky, I., Nathan, A., Donlin, L.T., Raychaudhuri, S., 2021. IFN-γ and TNF-α drive a CXCL10+ CCL2+ macrophage phenotype expanded in severe COVID-19 lungs and inflammatory diseases with tissue inflammation. Genome Med, 13, 64.

Zheng, J., Wang, Y., Li, K., Meyerholz, D.K., Allamargot, C., Perlman, S., 2021. Severe Acute Respiratory Syndrome Coronavirus 2-Induced Immune Activation and Death of Monocyte-Derived Human Macrophages and Dendritic Cells. J Infect Dis, 223, 785-795.

Zhou, P., Yang, X.L., Wang, X.G., Hu, B., Zhang, L., Zhang, W., Si, H.R., Zhu, Y., Li, B., Huang, C.L., Chen, H.D., Chen, J., Luo, Y., Guo, H., Jiang, R.D., Liu, M.Q., Chen, Y., Shen, X.R., Wang, X., Zheng, X.S., Zhao, K., Chen, Q.J., Deng, F., Liu, L.L., Yan, B., Zhan, F.X., Wang, Y.Y., Xiao, G.F., Shi, Z.L., 2020. A pneumonia outbreak associated with a new coronavirus of probable bat origin. Nature, 579, 270-273.

Zhou, Y., Zhou, B., Pache, L., Chang, M., Khodabakhshi, A.H., Tanaseichuk, O., Benner, C., Chanda, S.K., 2019. Metascape provides a biologist-oriented resource for the analysis of systems-level datasets. Nat Commun, 10, 1523.

Zhu, N., Wang, W., Liu, Z., Liang, C., Wang, W., Ye, F., Huang, B., Zhao, L., Wang, H., Zhou, W., Deng, Y., Mao, L., Su, C., Qiang, G., Jiang, T., Zhao, J., Wu, G., Song, J., Tan, W., 2020. Morphogenesis and cytopathic effect of SARS-CoV-2 infection in human airway epithelial cells. Nat Commun, 11, 3910.

549 **Figure legends**

550

551 **Fig. 1** SARS-CoV-2 induces MC degranulation and trachea lesions in hACE2-humanized mice. The mice of
552 C57BL/6N-ACE2$^{em2(hACE2\text{-}WPRE,\ pgk\text{-}puro)/CCLA}$ were intratracheally inoculated with SARS-CoV-2 (strain 107) at a
553 dose of $5 \times 10^6$ $TCID_{50}$. At day 5 post-infection, mice were anaesthetized and the trachea tissue were harvested
554 for histological analysis. Toluidine blue (T. blue) staining was used to observe MCs and degranulation (**A, C,**
555 **E**). Hematoxylin and Eosin (H.E.) staining was used to observe trachea injury (**B, D**). The PBS was used as the
556 mock infection (**A, B**). (**F**–**G**) The counts of MC and papillary hyperplasia in trachea section were summarized.
557 Scale bar: 100 or 20 μm. The number (n) of mouse used in tests was noted.

558

559 **Fig. 2** Transcriptome analysis of BEAS-2B cells. BEAS-2B cells were treated with the culture supernatants (the
560 sample "S") from SARS-CoV-2 spike/RBD protein-triggered LAD2 degranulation cells, or with the LAD2 cell
561 normal culture supernatants (the sample "M"), for 12 h. BEAS-2B cells were collected and the transcriptome
562 analysis was performed. The data summarized four independent experimental repeats. **A** Volcano plot of DEGs
563 comparing "S" versus "M" samples. The symbols of top 10 up-regulated and down-regulated genes are shown.
564 **B** GO functional enrichment analysis of DEGs. Color bar indicates minus logarithm of *q* values, and bubble
565 size indicates absolute gene counts enriched in GO terms. **C** GSEA of distribution of gene sets related to
566 inflammatory response, negative regulation of cell growth, viral life cycle and the enrichment scores based on
567 DEGs. **D** Transcription-factor enrichment analysis of DEGs. The color bar indicates the minus logarithm of *q*
568 values, and bubble size indicates the gene enrichment ratio regulated by a transcription factor. (**E**–**H**) Heatmaps
569 showing relative expression level (left panel), fold-change (middle panel), and adjusted *P*-values (right panel)
570 for sets of cytokine/chemokine-related genes (**E**), negative regulation of growth genes (**F**), cell adhesion (**G**),
571 viral life cycle (**H**).

572

573 **Fig.3** Blocking MC degranulation reduces the capacity to induce inflammatory factors in BEAS-2B cells.
574 BEAS-2B cells were treated with either LAD2/RBD co-culture supernatants (LAD2/RBD-supern.), LAD2 cell
575 culture supernatants (LAD2-supern.), or medium for 12h (**A**); or LAD2 cells were prior-treated with loratadine
576 (Lor., 5 μg/mL) or ebastine (Eba., 3 μg/mL) for 20 h, and then cells were treated with SARS-CoV-2 spike/RBD
577 (5 μg/mL) for 2 h, and the culture supernatants were harvested to treat BEAS-2B cells for additional 12 h (**B**).
578 The direct treatments of BEAS-2B cells with spike/RBD (5 μg/mL) or medium were also performed. The mRNA
579 levels of inflammatory factors were detected with real time qRT-PCR, and normalized to *gapdh* mRNA. One
580 representative data from 3 independent repeats are shown, data are mean± standard deviation (SD). $^{**}P < 0.01$, $^{***}P < 0.001$, and $^{***}P < 0.0001$ are considered significant differences in a Student's unpaired *t*-test.

582

583 **Fig.4** MC released mediators-induced expression of inflammatory factors. BEAS-2B cells ($2\times10^5$) were
584 stimulated with tryptase, chymase or histamine (5 μg/mL for each) for 12 h, and the cells were collected to

585 detect the mRNA levels of cytokines and chemokines. One representative data from 3 independent repeats are
586 shown, data are mean ± SD. ** $P<0.01$, *** $P < 0.001$, and **** $P < 0.0001$ are considered significant
587 differences in a Student's unpaired *t*-test.
588
589 **Fig. 5** The prior-treatment with loratadine and ebastine reduces SARS-CoV-2-mediated tracheal injury in mice.
590 The mice of C57BL/6N-ACE2$^{em2(hACE2\text{-}WPRE,\ pgk\text{-}puro)/CCLA}$ were infected intranasally with SARS-CoV-2 (strain
591 107) at a dose of $5\times10^6$ $TCID_{50}$ (**A**–**F**). The loratadine (Lor., 10 mg/kg) (**C, D**) or ebastine (Eba., 5 mg/kg) (**E,**
592 **F**) was administered one day before infection, and the treatments were continued daily throughout the infection
593 (five mice for each treatment groups). Mice were euthanized and trachea were harvested for pathological
594 analysis at 5 dpi. Toluidine blue (T. blue) staining (**A, C, E**) to observe MC degranulation, and Hematoxylin
595 and Eosin (H.E.) staining (**B, D, F**) to observe the trachea injury. **G, H** MC and papillary hyperplasia counts in
596 trachea sections were summarized. Scale bar: 100 μm. Data were presented as the summary from 5 mice in each
597 group. * $P < 0.05$ and ** $P < 0.01$ are considered significant differences in a Student's unpaired *t*-test.
598

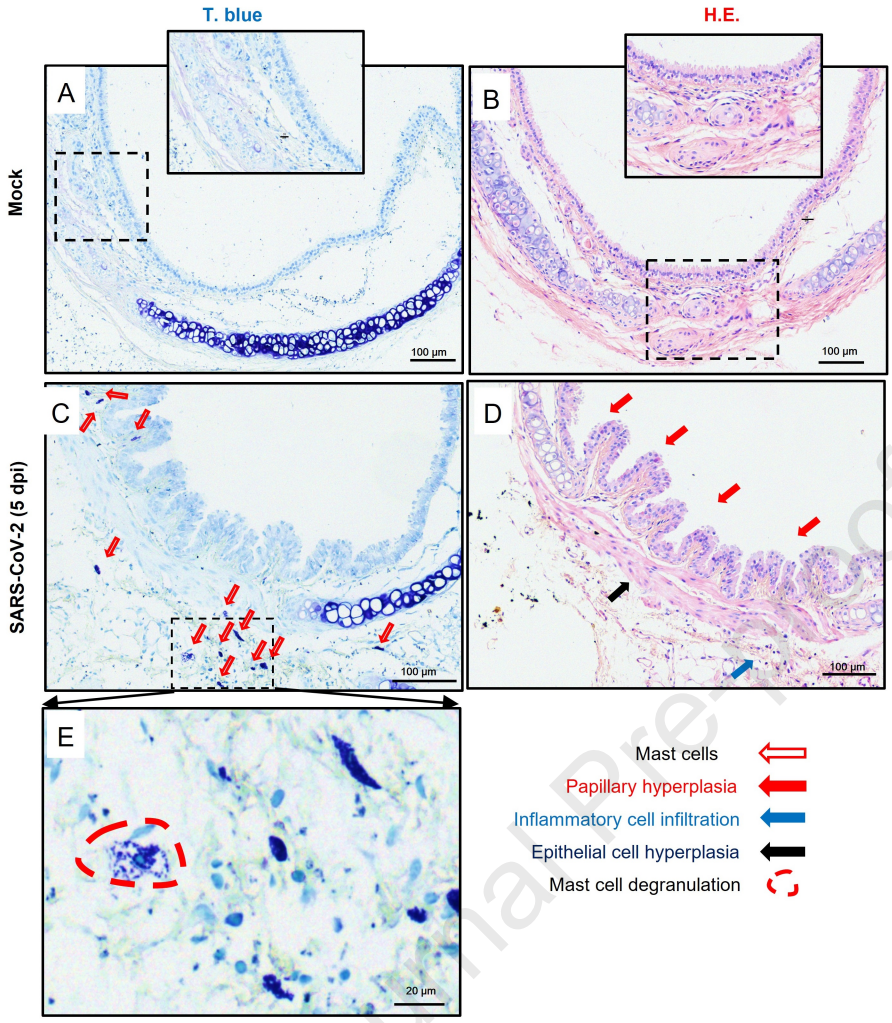


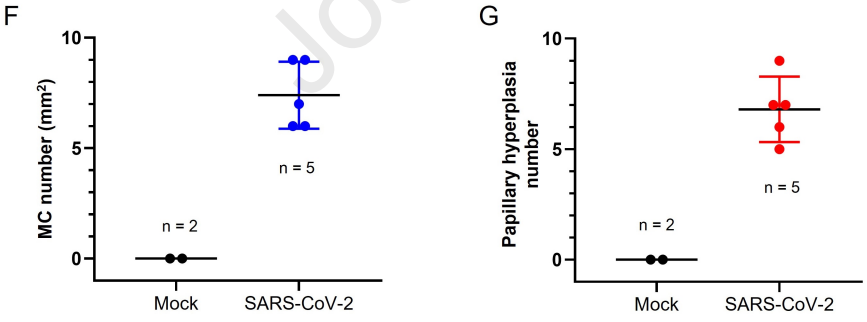

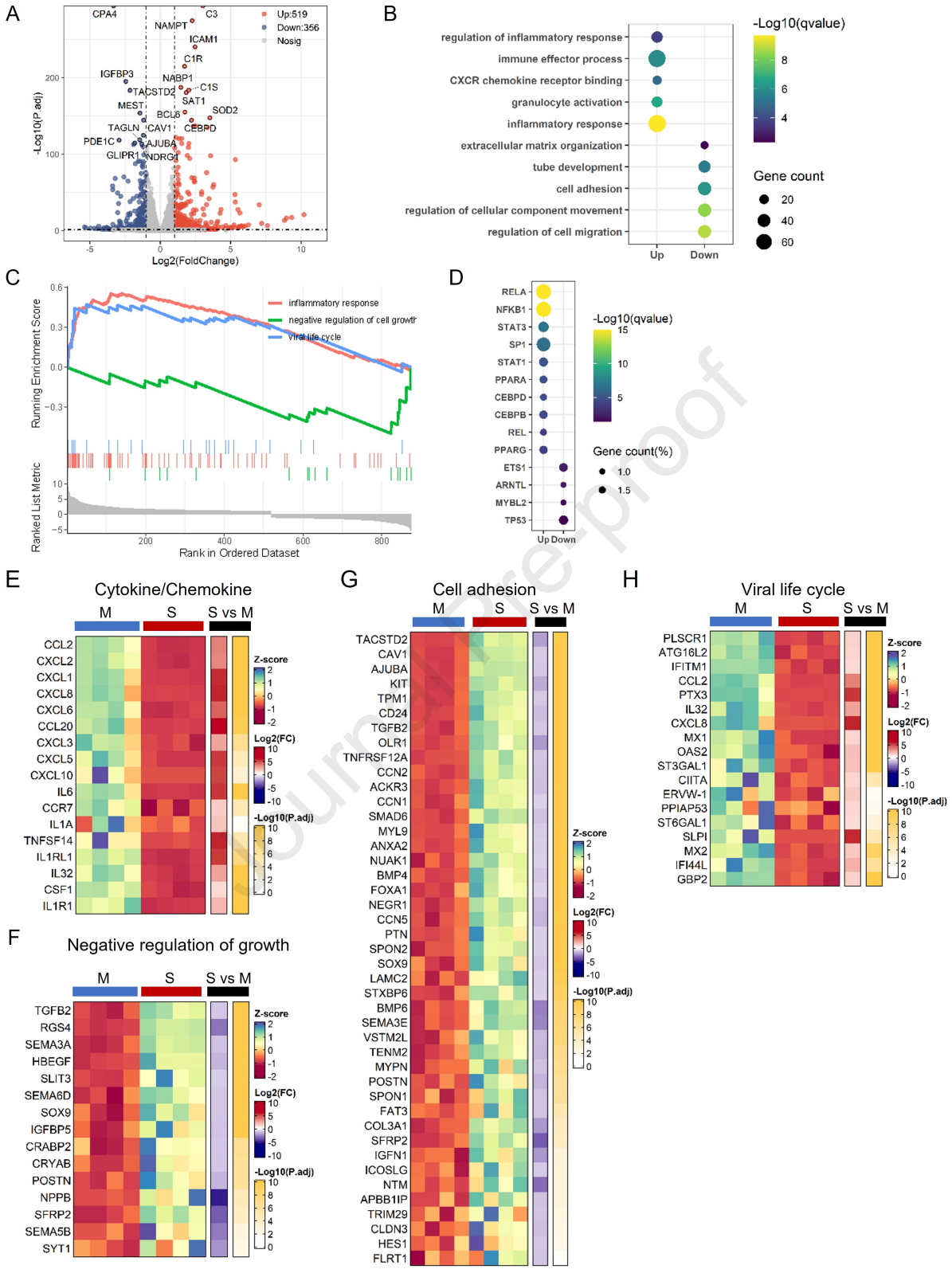

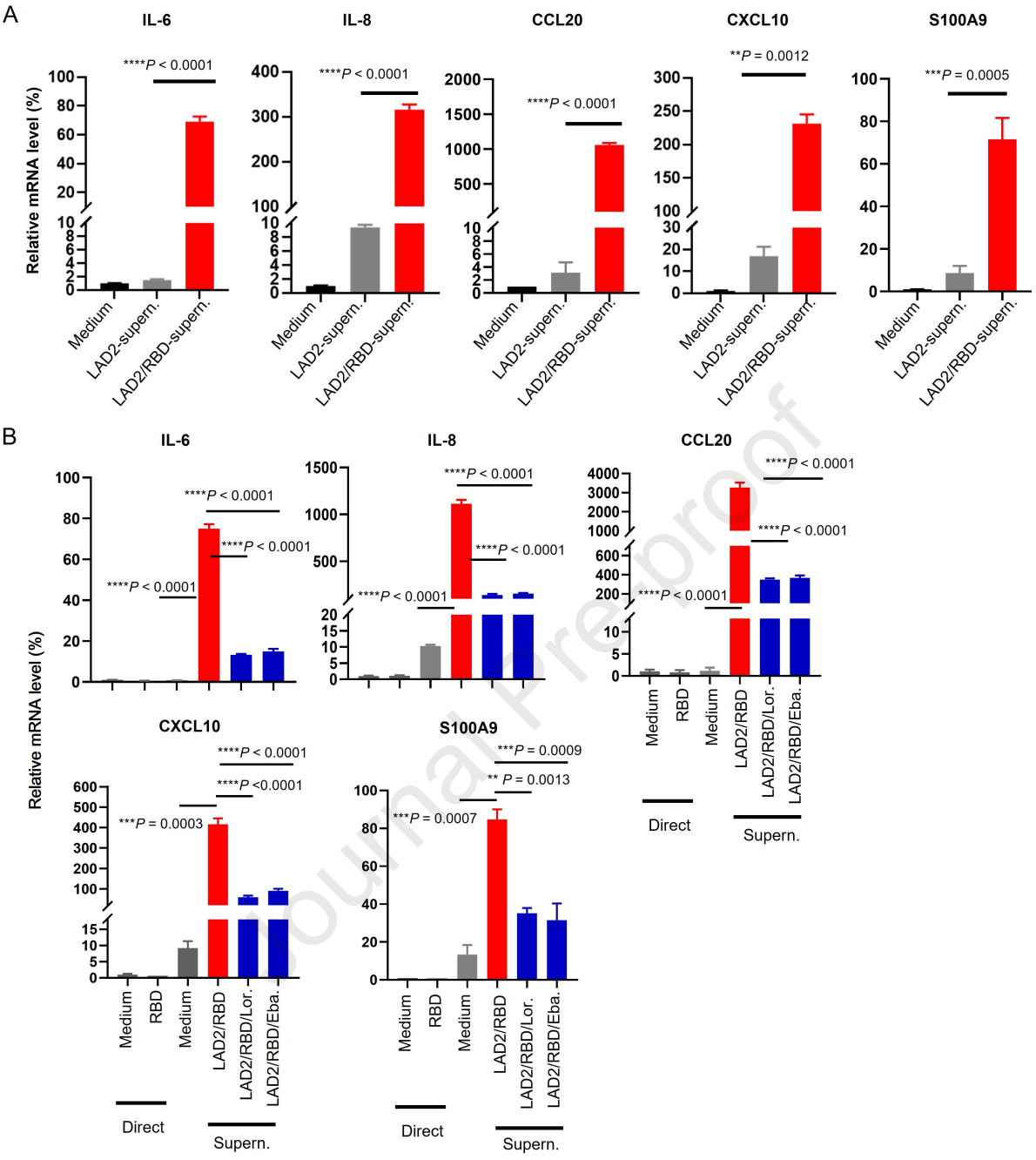

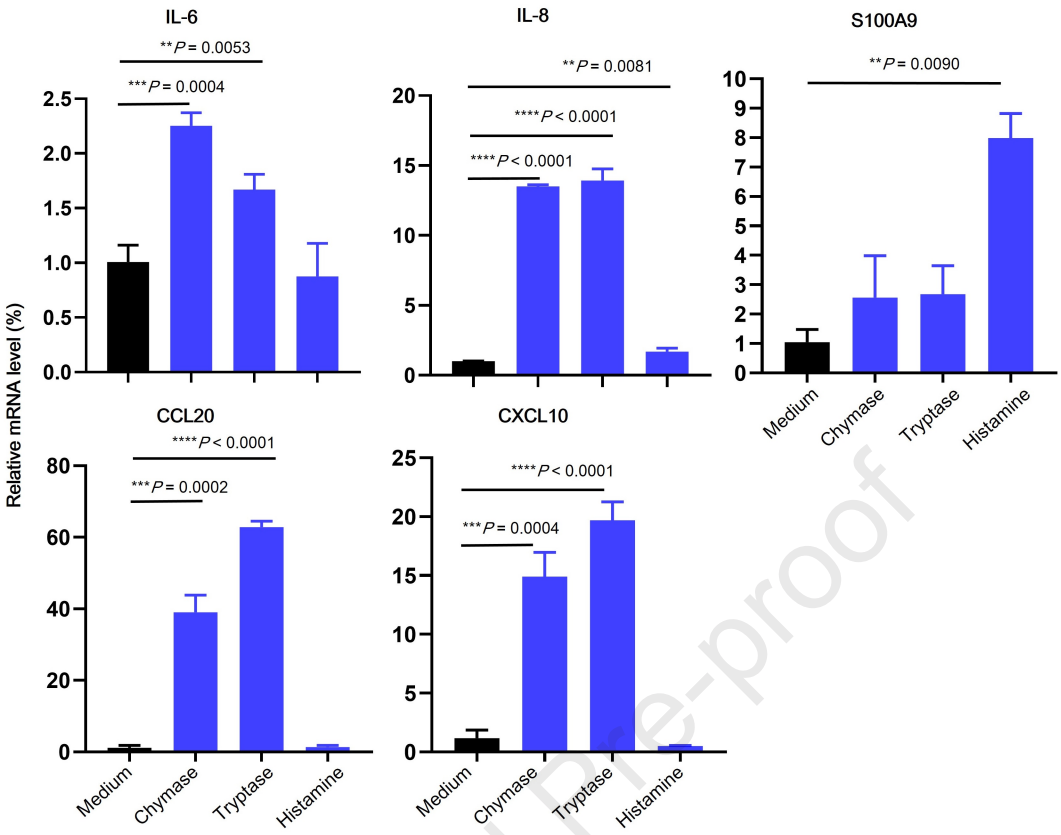

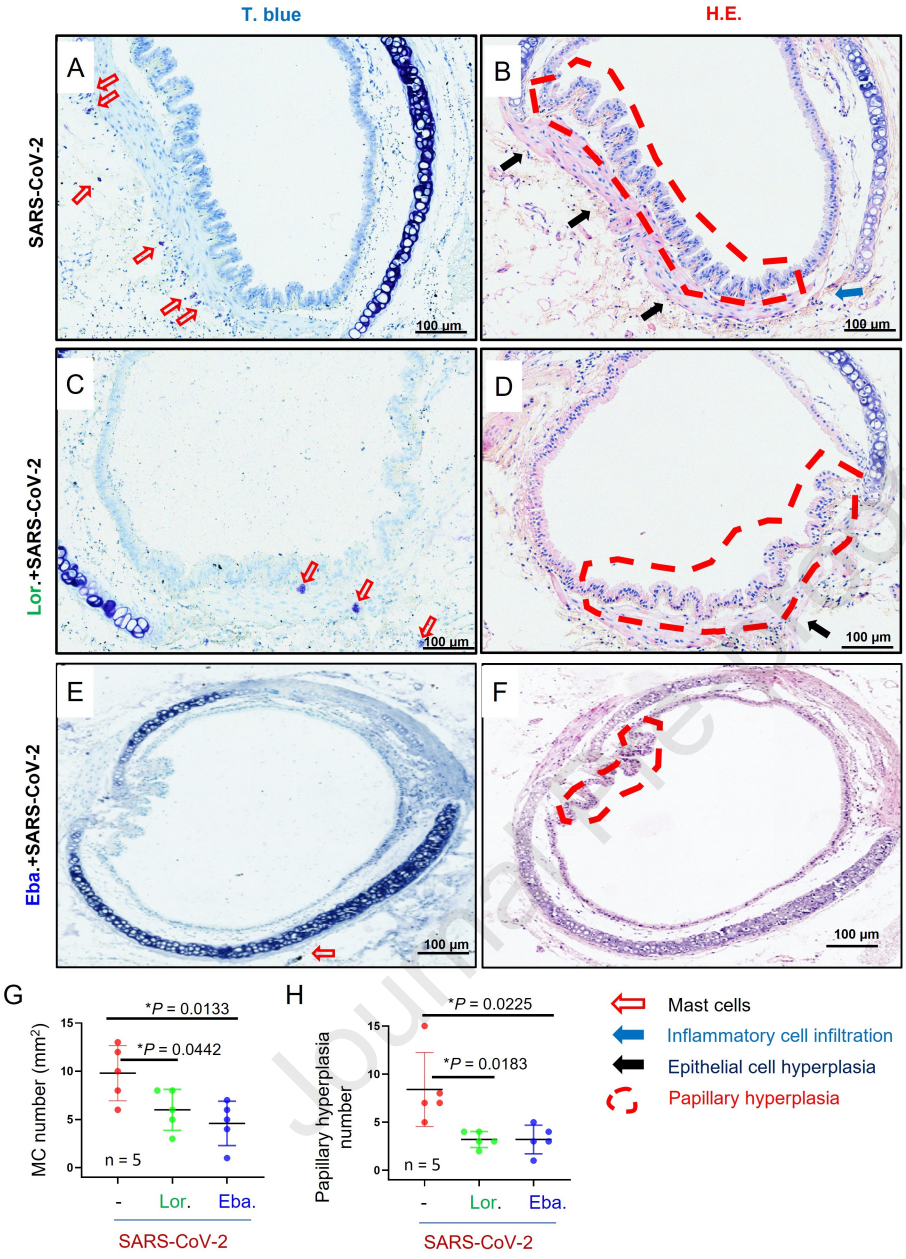
T. blue
H.E.
A
B
C
D
E
F
SARS-CoV-2
Lor.+SARS-CoV-2
Eba.+SARS-CoV-2
100 μm
G
MC number (mm²)
*P = 0.0133
*P = 0.0442
n = 5
-
Lor.
Eba.
SARS-CoV-2
H
Papillary hyperplasia number
*P = 0.0225
*P = 0.0183
n = 5
-
Lor.
Eba.
SARS-CoV-2
Mast cells
Inflammatory cell infiltration
Epithelial cell hyperplasia
Papillary hyperplasia